Analysis of the baryonic flux tube profiles in $N_f = 2$ lattice QCD at finite temperature.

V. G. Bornyakov[1], M. N. Chernodub[2], H. Ichie[3], Y. Koma[4],
Y. Mori[3], M. I. Polikarpov[2], G. Schierholz[5], H. Stüben[6] and T. Suzuki[3]

[1]Institute for High Energy Physics, RU-142284 Protvino, Russia
[2]ITEP, B.Cheremushkinskaya 25, RU-117259 Moscow, Russia
[3]Institute for Theoretical Physics, Kanazawa University, Kanazawa 920-1192, Japan
[4]Max-Planck-Institut für Physik, D-80805 München, Germany
[5]NIC/DESY Zeuthen, Platanenallee 6, D-15738 Zeuthen,
Deutsches Elektronen-Synchrotron DESY D-22603 Hamburg, Germany
[6]Konrad-Zuse-Zentrum für Informationstechnik Berlin, D-14195 Berlin, Germany

Lattice studies of the baryonic system consisting of three static quarks (3Q) are important for clarification of the baryon structure. Recently there appeared a number of papers devoted to the studies of the 3Q system at zero temperature [1, 2, 3]. It was concluded that the flux tube has a Y-shape, at least at large distances.

We study the flux tube profile in the baryonic system at finite temperature in QCD with dynamical fermions. The structure of the flux tube is investigated with the help of Abelian observables after the maximally Abelian gauge is fixed. In particular, we study the monopole and the photon parts of Abelian flux tube profiles. The Abelian and the monopole dominance phenomena are well established in the gluodynamics [4, 5]. Our study is also important to check the dual superconductor scenario of confinement which predicts that the effective infrared theory of QCD should be a kind of the dual Abelian Higgs model.

To study QCD with dynamical quarks we consider $N_f = 2$ flavors of degenerate quarks, using the Wilson gauge field action and non-perturbatively $\mathcal{O}(a)$ improved Wilson fermions [6]. Configurations are generated on the $16^3\,8$ lattice at $\beta = 5.2$, $0.1330 \le \kappa \le 0.1360$, corresponding to temperatures below and above the finite temperature transition at $\kappa_T = 0.1344$ ($T_c = 213(10)$ MeV) [7]. Details of the simulation can be found in [7]. We fixed the maximally Abelian (MA) gauge on generated configurations employing the simulated annealing algorithm [5]. The Abelian projection procedure [8] defines the diagonal link matrices $u^{\rm ab}_\mu(s) = {\rm diag}\{u^{\rm ab,1}_\mu(s), u^{\rm ab,2}_\mu(s), u^{\rm ab,3}_\mu(s)\}$, $u^{\rm ab,l}_\mu(s) = \exp[i\theta^{\rm ab,l}_\mu(s)]$, where $\theta^{\rm ab}_\mu(s)$ can in turn be decomposed into monopole (singular) and photon (regular) parts [9, 10]: $\theta^{{\rm ab},a}_\mu(s) = \theta^{{\rm mon},a}_\mu(s) + \theta^{{\rm ph},a}_\mu(s)$.

We study the Abelian action density $\rho_{\rm ab}(s)$, the Abelian color-electric field $E^a_j(s)$ and the monopole current $k^a_\mu(s)$. These are defined as

$$\rho_{\rm ab}(s) = \frac{\beta}{3}\sum_{\mu>\nu}\sum_a \cos(\bar\theta^a_{\mu\nu}(s)) \ , \quad E^a_j(s) = i\bar\theta^a_{j4}(s) \ , \quad k^a_\mu(s) = -\frac{i}{4\pi}\epsilon_{\mu\nu\rho\sigma}\partial_\nu\bar\theta^a_{\rho\sigma}(s+\hat\mu) \, .$$

We consider three types of Polyakov loop operators to create static sources: $L^{{\rm k},a}(\vec s) = \exp\left\{{\rm i}\sum_{t=1}^{L_t}\theta^{{\rm k},a}_4(\vec s, t)\right\}$, where $\theta^{\rm k}$ is $\theta^{\rm ab}$, $\theta^{\rm mon}$ or $\theta^{\rm ph}$.

The vacuum averages of our observables are defined for the baryonic case by

$$\langle\rho_{\rm ab}(s)\rangle_{3Q} = \frac{\langle\rho_{\rm ab}(s)\mathcal{P}_{3Q}(r_{\rm Y})\rangle}{\langle\mathcal{P}_{3Q}(r_{\rm Y})\rangle} - \langle\rho_{\rm ab}(s)\rangle, \quad \langle X_j(s)\rangle_{3Q} = \frac{\langle\frac{1}{3!}\sum_{a,b,c}|\varepsilon_{abc}|X^a_j(s)L^a(\vec s_1)L^b(\vec s_2)L^c(\vec s_3)\rangle}{\langle\mathcal{P}_{3Q}(r_{\rm Y})\rangle},$$

where $X^a_j(s)$ is $E^a_j(s)$ or $k^a_\mu(s)$, and $\mathcal{P}_{3Q}(r_{\rm Y}) = \frac{1}{3!}\sum_{a,b,c}|\varepsilon_{abc}|\,L^a(\vec s_1)L^b(\vec s_2)L^c(\vec s_3)$.

We discuss the structure of the baryonic flux tube in the confinement phase. Figure.1(a) shows the monopole and photon parts of the color electric field in the 3Q system. The monopole part is squeezed into a flux tube while the photon part is of Coulombic form. In the monopole component the flux tube is compatible with Y-shape. We expect that the agreement with Y-shape will be better when the distance between quarks will be large in comparison with the intrinsic width of the flux tube. The same conclusions can be drawn from the Figure.1(b) where the distribution of the monopole and photon parts of the action density is depicted. Figure.1(c) shows the monopole currents distribution. One can see circulating monopole currents around the color electric field in each slice. In the plane

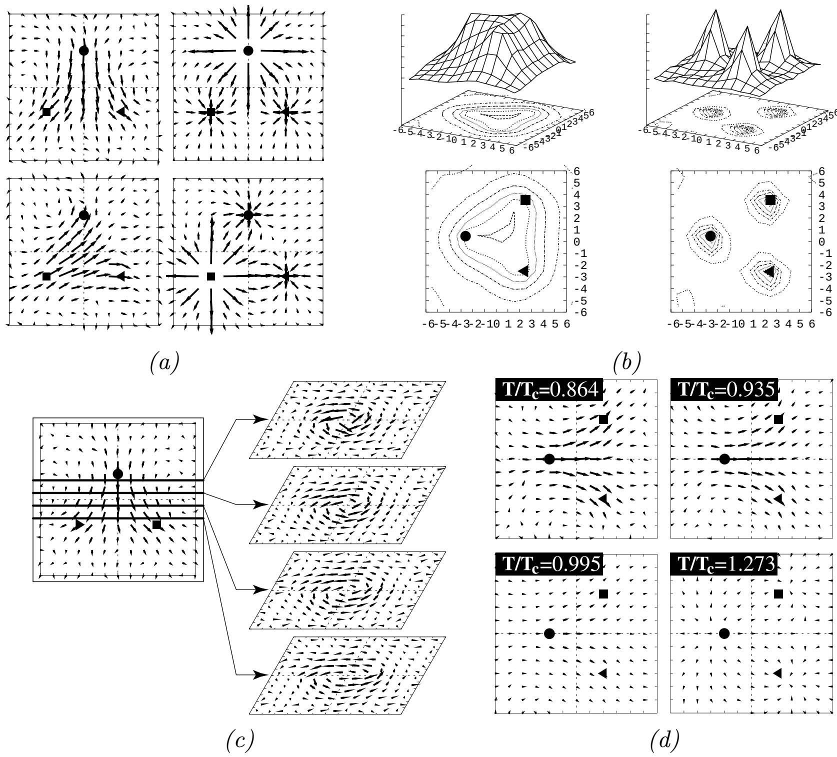

Figure 1: *(a) is the monopole (left column) and photon (right column) parts of the color electric field at* $T/T_c = 0.864$. *The color index of the color electric field coincides with that of the topmost quark (top row) or of the leftmost quark (bottom row). (b) is the monopole (left) and photon (right) parts of the action density at* $T/T_c = 0.935$ *and (c) is the monopole current (right), obtained from the monopole component of the Abelian gauge field at* $T/T_c = 0.864$. *(d) is evolution of the color electric field (monopole component) with temperature.*

where the color electric field is divided into two parts, the circulating monopole current is not a perfect circle anymore. This indicates a possibility of forming two circulating currents if the distance between quarks would be made larger.

And we show how the profile of the flux tube changes when the temperature increases and crosses over to the high temperature phase. From Figure.1(d) one can see that the squeezed color electric field (the monopole component) disappears at $T > T_c$. In contrast, the photon component of the color electric field, depicted in Figure.1(a)(right), does not show any essential changes when the temperature increases.

ACKNOWLEDGEMENTS

This work is supported by the SR8000 Supercomputer Project of High Energy Accelerator Research Organization (KEK). A part of numerical measurements has been done using NEC SX-5 at RCNP of Osaka University. T.S. is partially supported by JSPS Grant-in-Aid for Scientific Research on Priority Areas No.13135210 and (B) No.15340073. The Moscow group is partially supported by RFBR grants 02-02-17308, 01-02-17456, 00-15-96-786, grants INTAS–00-00111 DFG-RFBR 436 RUS 113/739/0, and CRDF awards RPI-2364-MO-02 and MO-011-0.

References

[1] C. Alexandrou, P. De Forcrand, A. Tsapalis, Phys. Rev. **D65** (2002) 054503
[2] T. T. Takahashi, H. Suganuma, Y. Nemoto, H. Matsufuru, Phys. Rev. **D65** (2002) 114509
[3] H. Ichie, V. Bornyakov, T. Streuer and G. Schierholz, Nucl. Phys. A **721** (2003) 899.
[4] T. Suzuki and I. Yotsuyanagi, Phys. Rev. D **42** (1990) 4257.
[5] G. S. Bali, V. Bornyakov, M. Muller-Preussker and K. Schilling, Phys. Rev. D **54** (1996) 2863
[6] S. Booth *et al.* [QCDSF-UKQCD collaboration], Phys. Lett. B **519** (2001) 229
[7] Y. Mori et al., Nucl. Phys. **A712** (2003) 930
[8] A. S. Kronfeld, G. Schierholz and U. J. Wiese, Nucl. Phys. **B293**, 461 (1987).
[9] T. Suzuki et al., Phys. Lett. **B347** (1995) 375; [Erratum-ibid. B **351** (1995) 603].
[10] J. Smit and A. van der Sijs, Nucl. Phys. **B355** (1991) 603.